

Features of Jets Formed by Erosive Capillary Discharges

A. Ya. Ender^{*,1}, V.I. Kuznetsov¹, I.N. Kolyshkin¹ and A.N. Shchetinina²

¹Ioffe Physical-Technical Institute, St. Petersburg 194021, Russia

²State Polytechnical University, St. Petersburg 195251, Russia

Abstract: An experimental study of the physical processes in a thin plasma jet produced by the pulsed discharges in the capillary with evaporated wall is described. The losses in mass from capillary wall as well as the transferred charge are accurately measured. The velocity of plasma jet propagation is measured, too. The current structure in plasma is studied. It is proved that a thin plasma jet can be obtained through capillary manufactured from not only polymer but also inorganic materials.

Keywords: Erosive capillary discharge, plasma jet.

1. INTRODUCTION

Ablation controlled plasmas are a special type of ultra-high density plasmas. They were obtained from a dielectric material in the air atmosphere for the first time in a high-power pulsed capillary discharge [1, 2]. Spectroscopic investigations have shown that the composition of the plasma inside a dielectric capillary is determined practically completely by the material of the inner wall of the dielectric. These investigations resulted in creation of the high-temperature sources of etalon radiation [3, 4]. The capillary discharge is widely used in soft x-ray lasers, extreme ultraviolet sources and laser-driven particle accelerators [5]. Such lasers, due to their present compactness, excellent beam quality and very reliable operation in wavelength range of 10–50 nm have become practical tools for high resolution microscopy, micro-holography, very high plasma density measurements, applications to semiconductor surface studies, and nano-lithography. Also, it supposed to apply such discharge for the electrothermal pulsed plasma thrusters, rocket propulsion, and hypersonic mass acceleration technology [6-12]. These thrusters have the combined advantages of system simplicity, high reliability, low average electric power requirement, and high specific impulse. They are considered as an attractive propulsion option for orbit insertion, drag makeup, and attitude control of small satellites. Besides, the capillary discharges can be used in the thin-film deposition [13, 14], in circuit breakers for switching-off higher currents [15-18], in electric fuses [19], and fireball modeling in laboratory [20-26]. In these devices, the discharge energy is dissipated by the ablation of the wall material, which then forms the main component of the discharge plasma.

In late 1980's, R. F. Avramenko *et al.* studied erosive discharges in capillary drilled in polymethylmethacrylate ($C_5H_8O_2$)_n (plexiglas) plate [20]. They discovered a thin

filament outflow of a dense kernel of a nearly capillary shape with diameter d and an adjacent bright plasma cloud (a shell). The special geometry of the discharge channel was a capillary in which one end was bounded by the carbon electrode and the other was kept free. In addition, a suitable scheme of the discharge circuit was applied. The jet has a length of about $100d$. Such a plasma jet exhibited no traces of divergence when it penetrates into a gas (pointing out the jet stability), long duration of its existence (of an order 10 ms) and high energy concentration. In Refs [20-22], the conditions how to initiate a thin plasma jet have been studied. The investigation of its structure and of the collisions with a target was also carried out. Particularly, it was shown that the plasma jet reacts with conductive materials and weakly interacts with the dielectric ones. The experimental results were independent on whether the metal plate was grounded or electrically isolated. The plasma was nearly quasi-neutral and its floating potential was not above 12 V.

Note that the jets are under observation in astrophysics (see, e. g., [23]). They are fairly stable configurations, being very similar in appearance to the plasma jets revealed in Ref. [20].

In recent years, the interest in erosive plasma jet concentrated on the description of its dynamics, being treated *via* different models [27, 28]. In Ref. [25], it was asserted that such plasma jet evolve in capillaries with polymer walls only. The authors of Ref. [28] advanced a model of the jet's structure. They assumed that the kernel consists of carbon particles of $\sim 10 \mu m$ -size which are due to evaporation of graphite cathode and of the electrons which were thermally emitted from their surface. In addition, a shell was formed by the vapor of the capillary wall material.

The authors in Ref. [27] divide jet generation and outflow process into four stages: breakdown, initial and quasi-stationary state, and decay. Under breakdown, a heating and evaporation of the capillary wall occurs. The current heats the gas resulting in a pressure growth and an jetting of the gas out of the capillary. At the initial stage, the

*Address correspondence to this author at the Ioffe Physical-Technical Institute, St. Petersburg 194021, Russia; Tel: +7 (812) 292-73-38; Fax: +7 (812) 297-10-17; E-mail: andrei.ender@mail.ioffe.ru

jet has a contact with the boundary separating the outflow gas and environment. Along the flow axis there is a narrow bright area (kernel) where plasma moves with a high velocity and has a high enthalpy. The shell density is significantly lower than the environmental gas density. First, the velocity of the tip of the jet in axial direction increases (up to 100 m/s , whereas in radial direction it is more than one order of magnitude slower), and then it decreases (this is the end of initial stage, where the current reaches its maximum). In the later stage the tip broadens becoming more spherical. At the quasi-stationary stage, the shell widens uniformly elsewhere. In the frontal spherical region a large scale gas motion arises. It conserves its stability for about tens *ms* after the termination of the current. The kernel length l can essentially change during a single discharge. In Ref. [27] an empirical formula for it was presented:

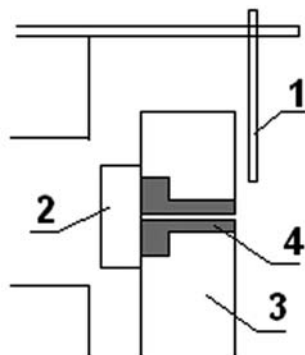
$$l(t)/d = 0.5i(t)/d^2. \quad (1)$$

Here, i is taken in Amperes, l in cm, and d in mm. It was claimed that this formula is valid only when current density in discharge channel is more than 10^4 A/cm^2 .

In spite of the many studies, the origin of the needle-like plasma jet as well as its stability remained unclear yet. Till now, no physical model has been advanced to describe the general features of such objects.

To approach the solution of above problem, it needs to accomplish a series of experimental studies. This work pursues those goals as follows.

1. To measure an amount of matter evaporated from the capillary walls as well as to measure the electric charge gone with a current during discharge time.
2. To measure the jet evolution in details. For this aim, it is necessary to record a jet structure with a high time resolution.
3. To gain a insight into the discharge current structure namely whether a current is shorting strictly against the second electrode, i. e. the jet being with no current, or, previously, the current goes along the jet and only then arrives at the second electrode by the reverse path. For this purpose, we place a metal target in the path of the jet located at different distances from capillary cut.



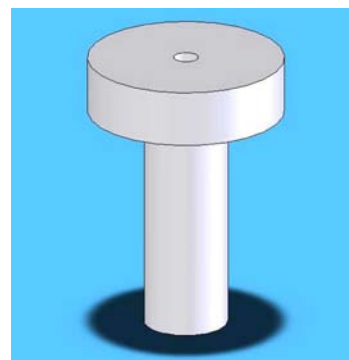
(a)

The paper is organized as follows. Sec. 2 describes the experimental setup and measurement techniques. Sec. 3 presents the results on the amount of material taken away from a capillary surface as well as of total electrical charge transferred with discharge current. As an important outcome the ratio of these values is advanced. In Sec. 4 the jet evolution during the discharge, with a high time resolution is shown, and jet front velocity is evaluated. To study the current structure, Sec. 5 present the results on jet interaction with a metal plate displayed perpendicularly to jet axis at different distances from the capillary cut. The effect of voltage polarity on a current structure is studied as well as the effect of a paper sheet covering the metal surface. The possibility to create a needle-like jet from the capillaries made from non-polymer materials is demonstrated in Sec. 6.

2. EXPERIMENT ORGANIZATION

To study parameters of the plasma jet formed in erosive capillary discharge, we made a setup realizing such a discharge. In Fig. (1a), it is shown the discharger's configuration. Sixteen capillaries were drilled circularly in the revolvable plexiglas disc. The capillary length is 10 mm . Such capillaries were drilled in small changeable muft, too. This construction of the capillary unit makes it possible to study the discharges in capillaries made from different materials and to measure the material mass loss with a good accuracy. In Fig. (2), an electric scheme for capillary discharge formation is shown.

For optical registration, we use Minolta DiIMAGE-5 camera with minimum exposition $500\ \mu\text{s}$ and VNC-748-H2 TV-camera with minimum exposition $0.5\ \mu\text{s}$. A system of optic registration of a jet with synchronization of the moments of a photo- or TV-camera exposition and the moment of capillary discharge ignition was developed. It makes possible the jet photo registration at different stages of its evolution. As the digital cameras have no option of their triggering by an external signal with a good accuracy, the discharge ignition needs to be related to any preliminary signal arising within these cameras. For flashing regime, Minolta has a preceding flash serving generally to determine auto exposition parameters including a power of main (second) flash which corresponds to shutter opening. The preceding flash is used to trigger a delay unit determining



(b)

Fig. (1). (a) Construction of the capillary discharger: (1) the return electrode (copper), (2) the feeding electrode (carbon), (3) the disk with holes, (4) the section of a changeable capillary. (b) Changeable plexiglas capillary.

moment of discharge ignition.

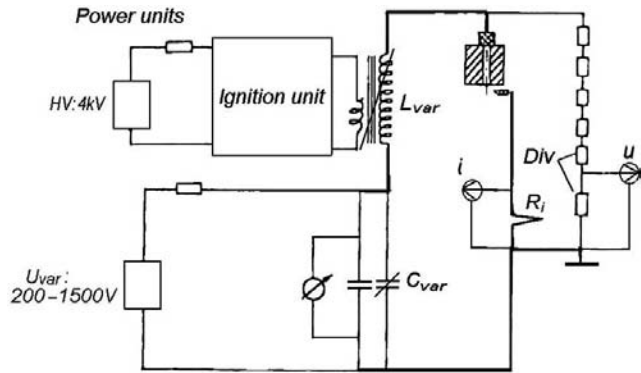


Fig. (2). Electrical circuit for investigation of the capillary discharge with evaporation wall. The high current contour consists of storage bank of capacities C_{var} , the secondary winding of the pulse transformer L_{var} , the discharger, and non-inductive shunt R_i . The diver Div is used for the voltage registration.

The VNC-748-H2 TV-camera continuously operates after switching on. But it has a short *Laser* signal to preliminary illumination with a delay from the end of the last exposition. It is regulated with a high accuracy by a code. In this case, the synchronization is simplified in compare with Minolta: de facto, it needs to form a single pulse which is synchronous with one of *Laser* pulses.

Both synchronization systems give the signals of the same type. They arrive to the experimental unit *via* the same channel with a galvanic decoupling. Involving the synchronization systems gives a possibility to carry out the jet registration at different stages of its evolution. For the illumination reduction, neutral filters of Russian HC type (Neutral Gray: "HC-8" reduced light of about 8 times, "HC-9" -- 50 times, "HC-10"-- 285 times) were used.

The discharge ignition happens as follows (see, Fig. 2). Primarily, a storage battery of $C = 0.06 - 0.51$ mF capacity and a high-voltage capacitor of ignition unit are charged up to a voltage of about 1 kV and to 4 kV, respectively. Then, using a short signal activating the ignition unit, a high-voltage pulse is formed which ignites a spark in the capillary. An inductance L of a secondary coil of pulse transformer is placed between the battery and carbon electrode. This inductance can be varied from 0.8 mH to

6.87 mH. If the storage battery is charged up to sufficient voltage, a current i through the inductance begins to increase with an arc discharge forming in the capillary. The discharge is accompanied by wall evaporation and plasma jet from open end of the capillary.

The oscillograms of a current i and discharge voltage u are recorded with digital memory oscillograph C9-8 and then the oscillograms are passed to a computer. A typical example of such oscillograms is shown in Fig. (3). One can see that a current is as high as hundreds Ampere and a voltage -- hundreds Volt. A discharge current exists about 2 ms at minimum inductance. In Fig. (4), an integral photo of jet from the digital camera Minolta Dimage-5 is shown. Here jet length is approximately 20 cm.

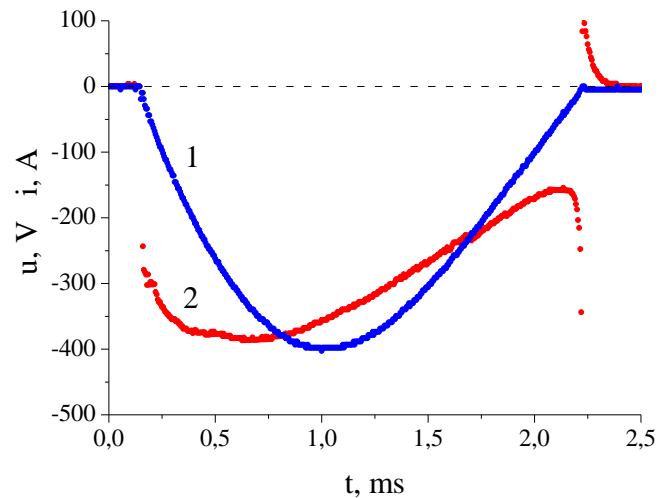


Fig. (3). Oscillograms of (curve 1) the discharge current and (2) the voltage. The inductance $L = 0.81$ mH, the capillary diameter $d = 1.5$ mm, the storage voltage $U = -1.2$ kV.

3. MEASUREMENT OF MASS REMOVED FROM CAPILLARY WALL

Earlier, an amount of the matter evaporated from the dielectric capillary surface with discharge was measured experimentally or estimated on a basis of the different models in a series of work. E.g., for polyethylene capillaries,

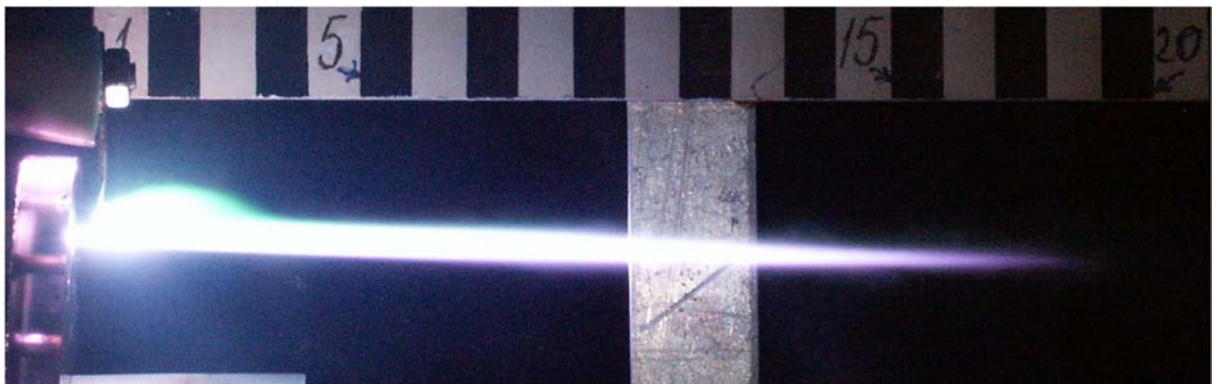


Fig. (4). Example of the jet integral photo: filter HC-9, the aperture number is 8.

it was accomplished in Refs. [8, 12, 30], and for Teflon capillaries -- in Refs. [7, 16, 31]. However, in these papers, the plasma jet was not thin, energy supplied into discharge was significantly higher, and a pulse duration was much shorter than in the experiments with a thin plasma jet. There is no precise data on an amount of matter lost from capillary surface with discharge in the thin jet. E.g., in Ref. [20], an average flow of erosive products of plexiglas wall was estimated as $(10 - 50) g cm^{-2} s^{-1}$.

We have measured the change in mass. For this purpose, we used a small capillary plexiglas module about 200 mg mass, shown in Fig. (1b). A hole of the same shape as this module was drilled in the disk (Fig. 1a). A lost mass Δm was determined by weighting the changeable modules pre- and after the discharge with analytical balance with an accuracy of 50 μg . This yielded an accuracy to be not worse than 5%. The mass lost Δm turned out to be of order 1 mg.

It is known, that there is a relation between the evaporation rate \dot{m} of the material of the metal cathode and a current I at the cathode: $\dot{m} = \mu_k I$ in vacuum arcs, a coefficient μ_k being $(0.5 - 1) \cdot 10^{-4} g/C$ depending on the cathode material [32]. We measured the electric charge q gone with a current during discharge time t_p , too. It was calculated as follows:

$$q = \int_0^{t_p} i(t) dt. \quad (2)$$

The q --magnitude was about 1 C.

Basing on the literature data we can assume that a temperature of the capillary discharge plasma is about 10000 K. In this case almost all the atoms have to be in an ionized state. In this connection we calculated a value $q/\Delta m$. It is about $10^3 C/g$. We estimated a value of the similar ratio also for the capillary discharges under study in Refs. [8, 12, 30]. We calculate a charge q integrating a discharge current along the pulse duration. A ratio $q/\Delta m$ turns out to be a rather below as compared with our case: of the order of $0.1 \cdot 10^3 C/g$. As it was noted above, the discharge conditions in these works distinct well from conditions of our discharge.

We assume that average molar mass in a plasma is $M = 15$ for our discharge. Then a value $f = Mq/\Delta m$ reaches $15 \cdot 10^3 C/mol$. Compare this value with the Faraday number F used in electrolysis calculation. Remember, that the Faraday number is a charge needed to deposit one gram-equivalent of matter, and numerically is a product of the electron charge e and the Avogadro number N_A , so $F = eN_A = 96.5 \cdot 10^3 C/mol$. Introduce a ratio $\alpha = f/F$. For our case, α is about 10%. Also, we measure the escaped mass and charge for the capillaries made from

non-polymer materials with the same dimensions as the plexiglas one (see, Sec. 6.) In this case, a value α is about several percent. We reveal that a coefficient f related the lost mass and transferred charge equals several percent of the Faraday number. Certainly, this coefficient is not a universal constant and is changed with the discharge conditions but not in large amount. It was found that f depends on a storage voltage U , a diameter d , and a capillary wall material. The experiments for a series of U were accomplished, U being varied within the range $0.5 kV - 1.2 kV$. The storage capacity was $0.5 mF$.

After each "shot", a capillary diameter increases due to evaporation of matter from its wall. A capillary cross section is near the circular one. The diameter was determined with a microscope as well as *via* the change in capillary mass considering the material density (the plexiglas density $\rho = 1.19 g/cm^3$). The dependencies Δm on d for two series of experiments at a storage voltage $U = 1.2 kV$ on a capacity of $0.5 mF$ with the circuit inductance $L = 0.8 mH$ are shown in Fig. (5a). Here, previously the dependencies Δm on the shot number was approximated *via* a polynomial with the least-square method to smooth them. Each series was accomplished with a new specimen of capillary of different diameters. The mass losses decrease with an increase in capillary diameter. A mean specific rate of losses in the erosive products of capillary wall is $(0.3 - 3) g cm^{-2} s^{-1}$, being about 1.5-order smaller than the estimations in Ref. [20]. From the other side, the data of our measurements turn out to be near to that from Refs. [8, 30], where specific mass loss of the polyethylene capillary wall was $(2 - 4) g cm^{-2} s^{-1}$.

A jet can also contain the particles from end electrode (carbon as a rule). Our electrode is a cylinder slab of 5 mm in diameter and about 0.5 g in weight. After ten shots, electrode mass loss is below 0.5 mg, which is far less than the capillary wall loss. So the electrode material seems to be of minor importance for the discharge properties, and, as we suppose, the plasma formation mechanism advanced by authors [28] is dubious.

A dependence of the charge gone with a current during discharge time on a capillary diameter is shown in Fig. (5b). A charge increases with the diameter growth. Fig. (5c) shows dependencies of the ratio $q/\Delta m$ on d for two series of experiments. One can see that these dependencies practically coincide in a region of diameters overlapping. It demonstrates a good reproducibility of the results. A value $q/\Delta m$ increases with the capillary diameter growth.

When fixing a capillary diameter d , both the outgoing mass and charge growth with an increase in supplied voltage. It is shown in Fig. (6a, b) where such dependences are built-up as a function on a storage voltage U for two values of capillary diameter. When this voltage is doubled, Δm and q increase in 3-4 times, whereas a ratio $q/\Delta m$ decreasing more weakly -- on (20 - 25)% (Fig. 6c).

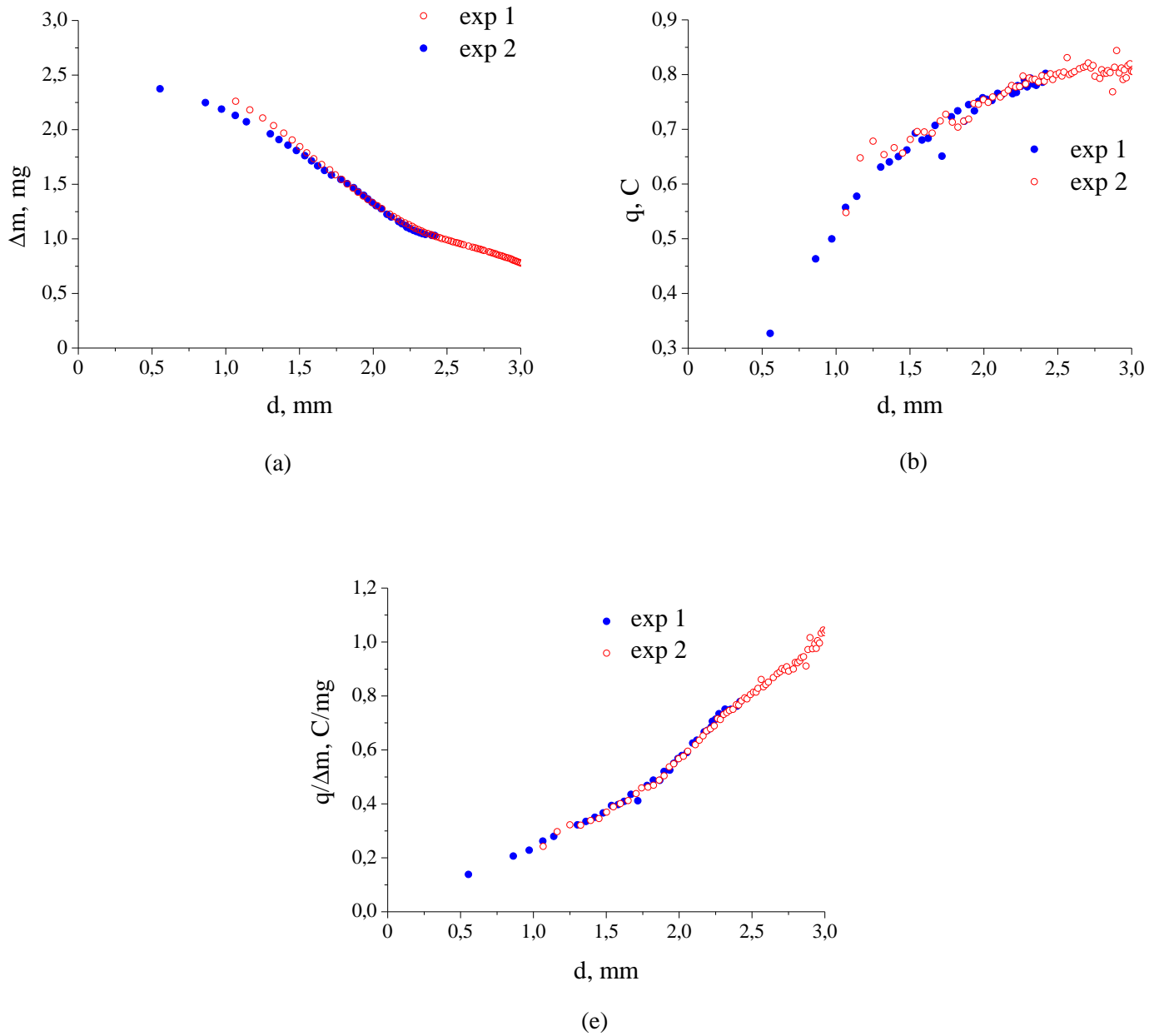


Fig. (5). Plots of (a) Δm , (b) q and (c) the ratio $q/\Delta m$ vs the capillary diameter for two series of experiments; $U = -1.2kV$.

Using the time-dependences of the current i and discharge voltage u , we calculated the energy E released in a discharge:

$$E = \int_0^t i(t)u(t)dt, \quad (3)$$

Fig. (7) shows the dependence of this energy on the capillary diameter. It is seen that a value E changes within 300 J -- 150 J range decreasing when the diameter increases.

4. JET EVOLUTION

We carried out the visual study of the jet evolution during the discharge current. A digital camera Minolta Dimage-5 was used. Both the jet's integral pictures and the

pictures with minimum exposure (0.5ms) for different time delays relatively to the discharge initiation were carried out. A change of jet's shape at different time delays is presented in Fig. (8). A time delay is estimated as a time lag of main (second) flash relative to the moment of discharge ignition.

With minimum inductance ($L = 0.8 mH$) we were able to vary the storage capacity voltage in a wide range. Therefore the processes with the high time resolution were generally studied with $L = 0.8 mH$ (Fig. 8b). The discharge time was about 2ms (a series of photos in Fig. 8d) at such parameters of the discharge circuit ($C = 0.5 mF$ and $L = 0.8 mH$). At the maximum inductance ($L = 6.87 mH$, Fig. 8a) the discharge time is higher (up to 6ms) (a series of photos in Fig. 8c). Comparing these series, one can see that the jet becomes more diffused with an increase in the

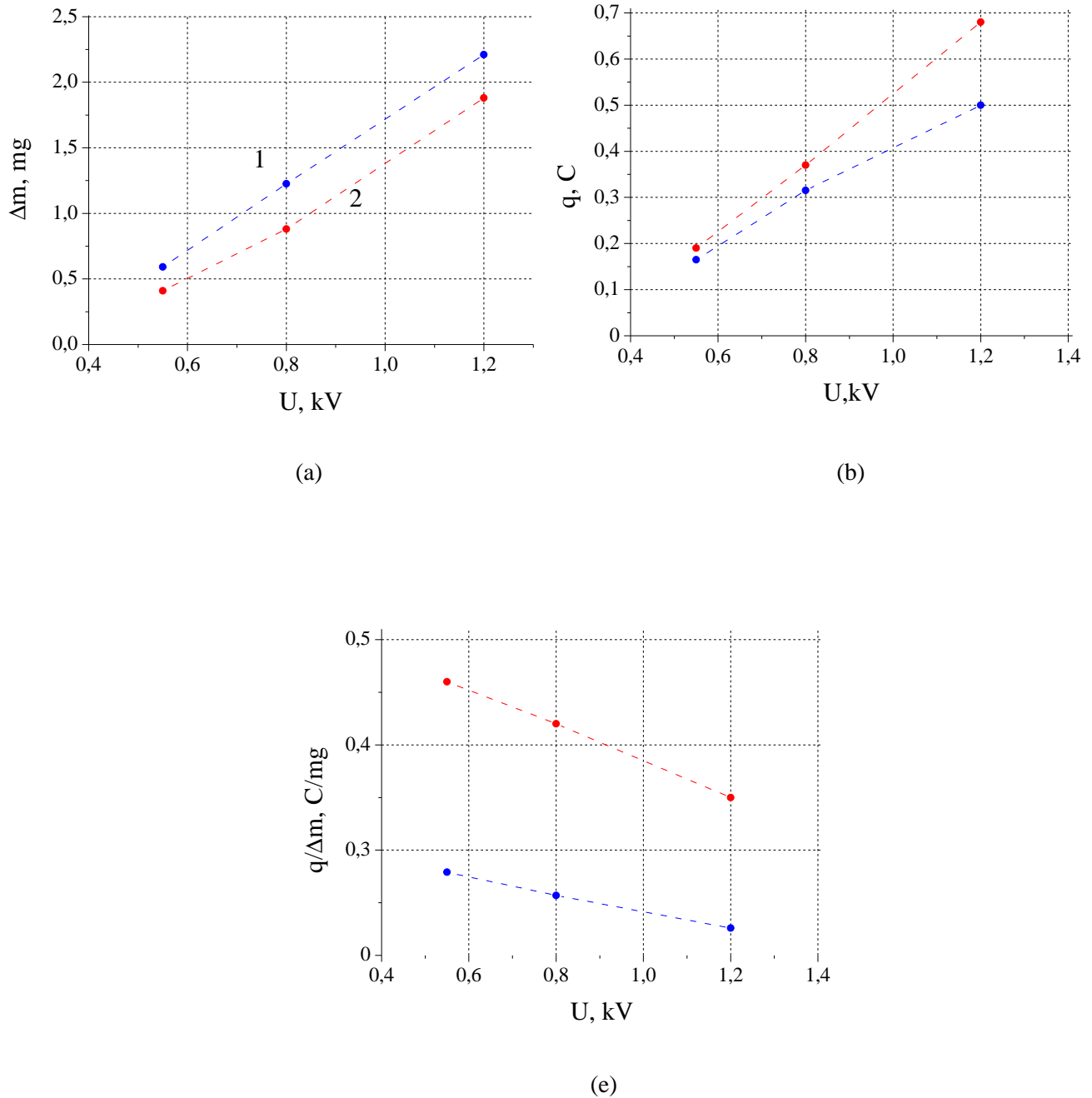


Fig. (6). Plots of (a) Δm , (b) q and (c) the ratio $q/\Delta m$ vs the storage voltage U : (curve 1) the capillary diameter $d = 1mm$, (2) 1.5.

discharge power, but its propagation velocity increases. The estimations of plasma jet propagation velocity in air for the case referring to Fig. (8a) turns out to be in $(30 - 100) m/s$ range, and to Fig. (8b) - $(100 - 250) m/s$.

A visual length of intense luminous central part (kernel) of the jet increases during current rises (and some more due to the jet inertia). Then it begins to decrease. The reduction of this part of the jet was observed for the first time. A kernel length estimated from presented photos is well described in a region of large currents by an empirical formula:

$$l(t) \approx 0.11 \cdot i(t) / U^{5/2} d. \tag{4}$$

Here, i is given in Amperes, U in kilovolts, d in mm, and l in cm. Note, that this formula, advanced in Ref. [27], depicts well a kernel length as a function of current and voltage stored, contrary to Eq. (1) which underestimates l by 20% for $U = 0.5 kV$, and 7 times overestimates it for $U = 1.2 kV$.

To observe details of rapid jet, we carried out a number of shots with VNC-748-H2 TV-camera, which has higher

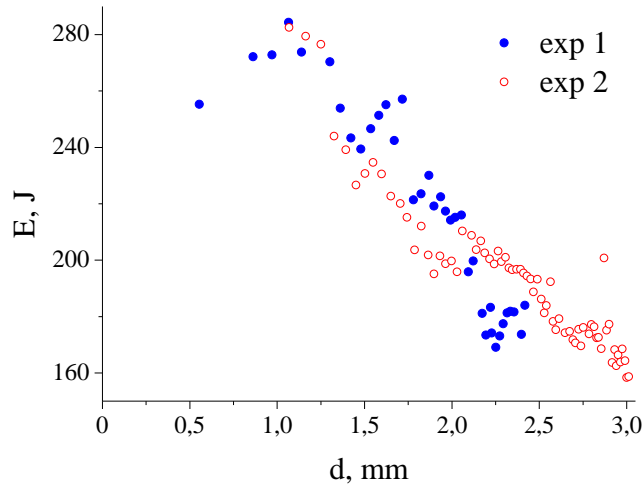
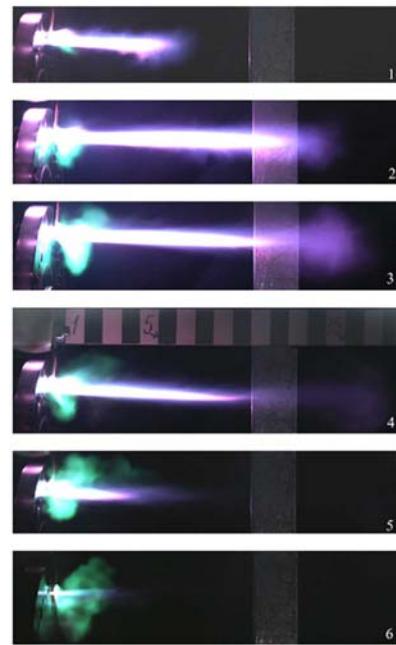
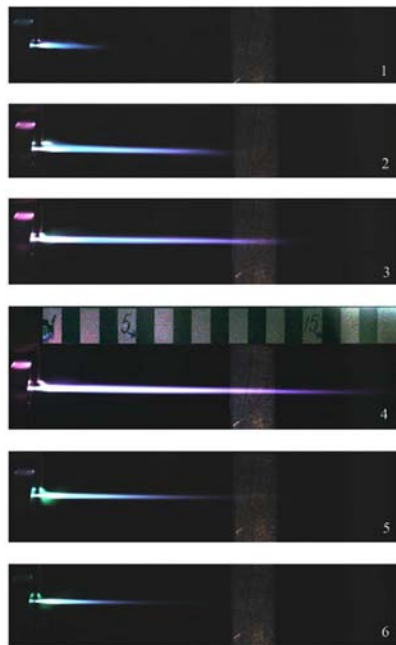
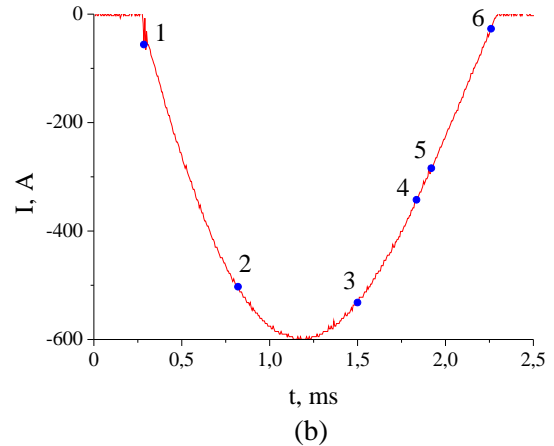
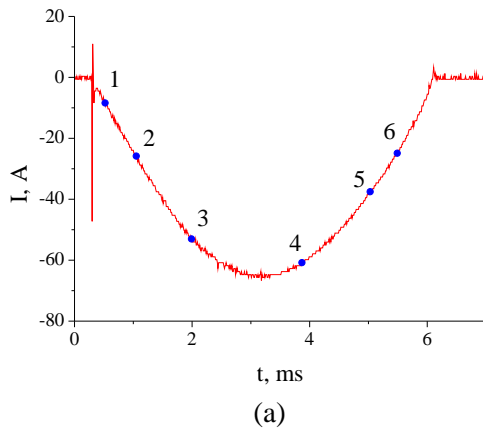


Fig. (7). Plots of the discharge energy vs the capillary diameter for two series of experiments; the storage energy is constant. $U = -1.2kV$.

time resolution than Minolta. In Fig. (9), it is shown the different stages of a plasma jet evolution. Here, a path of reverse current is well seen as it does not displace during exposition time. It should be noted that VNC-748-H2 TV-camera, but not a photo-camera, gives a possibility to see near infrared radiation, i. e., to reveal the jet's behaviour even after the end of a pulse of a current. However, the present article does not treat this stage. The results of a quantitative study of current structure are presented in the next Section.

5. INTERACTION OF THE JET WITH TARGET

Ref. [20] treats the interaction of a thin plasma jet generated by erosive discharge in the capillary with a metal target. Particularly, it was obtained the effective pictures of jet interaction with a thin gold foil. Pitifully, it is not so clear whether a current went through the metal foil or not. The foil destruction can occur due to large currents. Then, the experiments in Ref. [20] could simulate the wire explosion effect.



(e)

(f)

Fig. (8). Change in the jet form for various values of the delay time t_R . Filter HC-9. Numbering of the pictures corresponds to digits on relevant curve $i(t)$: (a) and (c) $d = 2.2mm$, $U = -0.5kV$; $L = 6.87mH$: (photo 1) $t_R = 0.515ms$; (2) 1.045; (3) 1.991; (4) 3.865; (5) 5.030; (6) 5.490. (b) and (d) $d = 2.5mm$, $U = -1.2kV$; $L = 0.809mH$: (photo 1) $t_R = 0.05ms$; (2) 0.54; (3) 1.22; (4) 1.555; (5) 1.67; (6) 1.98.

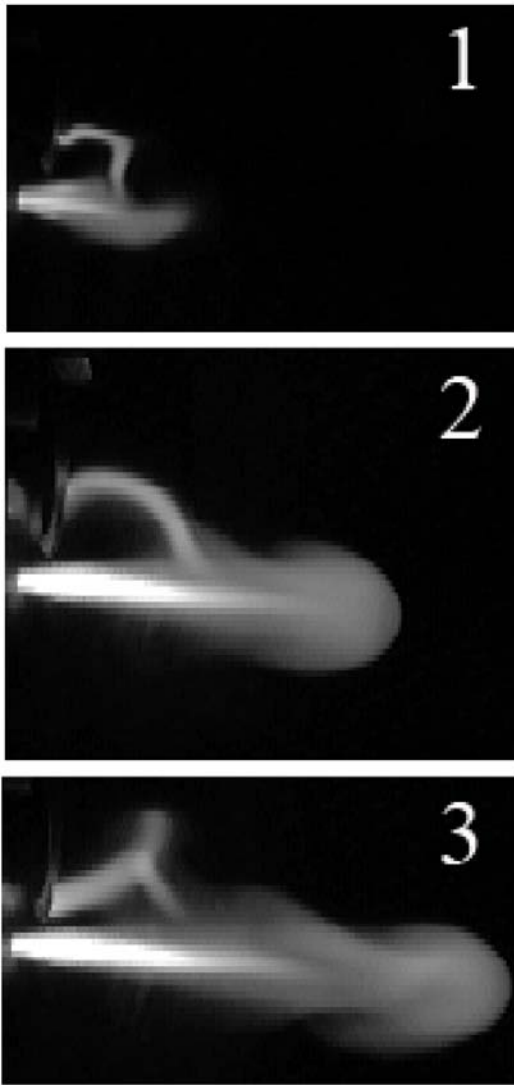


Fig. (9). Changing in the jet form for various values of the delay times: (1) $t_r = 0.8ms$, (2) 1.5, (3) 2.0. $d = 2.2mm$, $U = +0.65kV$, $L = 6.87mH$; the exposition $0.5\mu s$, filter HC-8.

We have been able to determine the current distribution along the jet in our experiments. When a current goes through a metal target, this distribution can be seen by changing the position of the metal target relative to the capillary cut. When discussing the current distribution through the jet, we advance a hypothesis that the current flows within the kernel in forward direction, and returns to the reverse electrode through the surrounding shell. An analogous hypothesis on the mechanism of jet's current was advanced in Ref. [27]. If our hypothesis is valid, some part of the current (or a whole current) goes through the grounded plate, when the jet strikes this plate, and a current in the main circuit decreases (down to zero). It needs to examine this hypothesis experimentally. To measure the current of the main circuit with no bypass of the current through the plate, the plate was removed and a shot was carried out in free space. Thus, the study of the currents in the main circuit and the plate circuit gives an opportunity to study the current structure of jet in details.

When studying the current structure of a plasma jet as well as plasma interaction with the metal targets, a metal plate (target) of $(2-3)mm$ thickness was put perpendicularly to jet's path at different distances l from capillary cut, being grounded through a shunt $3.75m\Omega$. A storage voltage U was from $700V$ to $1200V$. Supplied voltage was either the positive or negative polarity. The jet was fixed with VNC-748-H2 TV-camera. A time delay t_r , i. e., a lag of the "electron shutter" opening relative to discharge ignition, was varied within $0.5ms-4ms$ range, and an exposure time as a rule was minimal ($0.5\mu s$). HC-9 filter was used to reduce brightness. Under interaction of plasma jet with the metal plate, welding and destruction of metal occurs (see Fig. 10). A circular crater arises on a metal. Its diameter and depth depend on energy supply to the discharge and a distance of the plate from capillary cut. As a rule, the crater diameter is larger than the capillary one. A steel $1mm$ thick plate is perforated after several shots. The outlet hole is usually smaller than the capillary diameter. Any important effect of the plate grounding, as well as polarity of supplied voltage, on metal disruption was not seen. The condensed droplets of metal precipitate forming a rather wide circular grid structure on the crater edge. One can see the heat colors circles outside this structure. Sometimes, rather long radial "rays" of darker material than metal surface are seen.

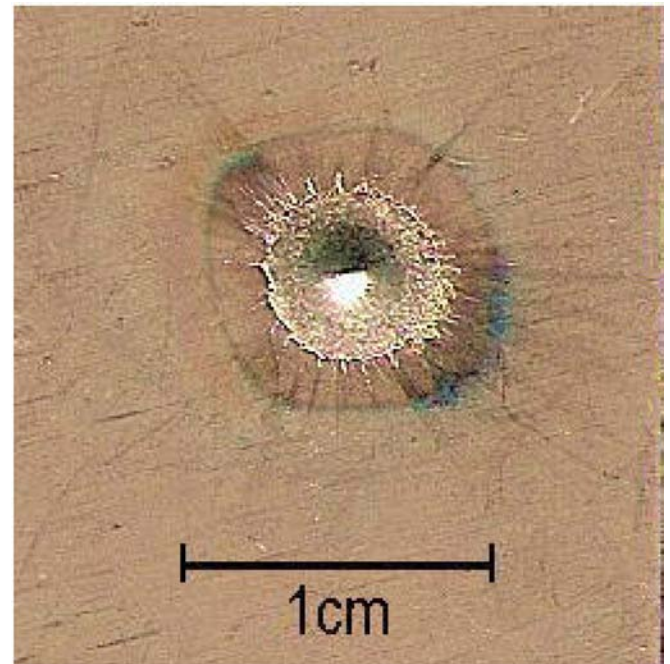


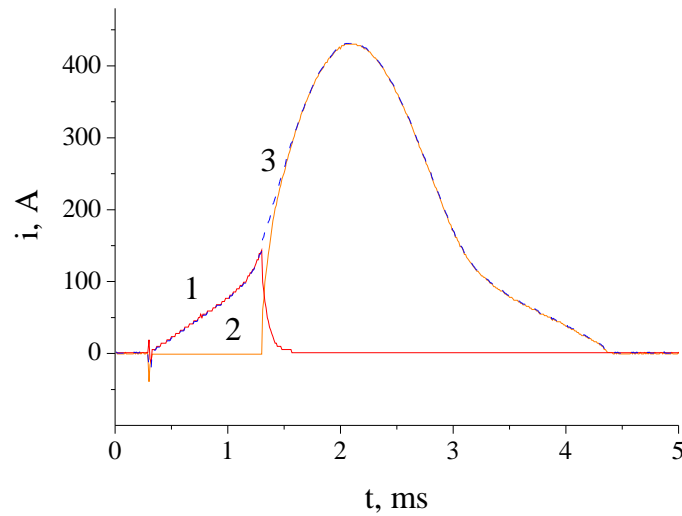
Fig. (10). Crater on metallic target after the plasma jet shock. $U = -750V$, the capillary diameter $d = 2mm$, the distance to the target $l = 30mm$.

Further, we carried out series of experiments, measuring simultaneously a current in the main circuit and that in circuit of a plate (remind that the plate may be grounded *via* the special shunt). When voltage on the feeding electrode is positive, a whole current changes over to the target as a rule,

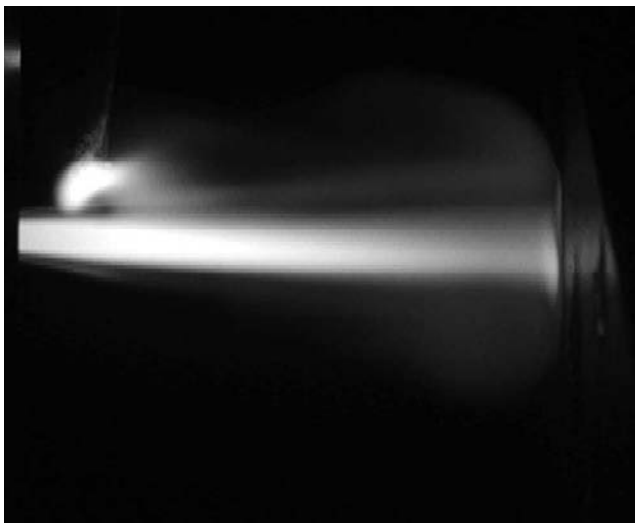
and the current in the main circuit vanishes (see, Fig. **11a**). The current changes over with a time lag t_r . The lag value depends on the target position. Process of current change-over is rather rapid (less than $100 \mu s$). Fig. **(11b)** shows an example of a jet's phase at a time shorter than $t_r \approx 1.1 ms$. In this case, a whole reverse current goes *via* a return electrode being accompanied by an intense brightening near this electrode. If the delay is longer than t_r , there is no current through the return electrode as well as luminosity near it (Fig. **11c**), i.e. whole current does go to the plate.

It should be noted that sometime the oscillations of current occur when there is no change in voltage and circuit parameters. E.g., in Fig. **(12a)**, these dependences are shown for the same parameters as in Fig. **(11a)**. Although each current oscillates, the time dependence of a sum current is smooth. The relevant photo of the jet is shown in Fig. **(12b)**. One can see the differences from Fig. **(11b)**.

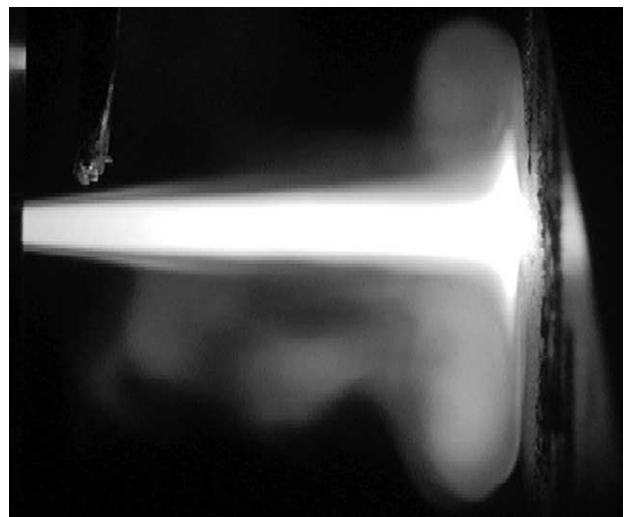
As a rule, for negative U an incomplete current switches to a target occurs (Fig. **13a**). In Fig. **(13b)**, the relevant jet photo with $2 ms$ delay is presented, when the plate was already touched. A current onto return electrode is seen clearly. In Fig. **(13a)**, one can see that the time dependence of a whole current is smooth, although each current has the



(a)



(d)



(e)

Fig. (11). (a) Current distribution in the case of grounded metallic target: (yellow curve) the target current, (red) the current in main circuit, (dashed) the sum current; $L = 6.87 mH$, $d \approx 3 mm$, $U = +1 kV$; $l = 28 mm$. TV-camera jet photos: (b) $t_r = 1.08 ms$, (c) 1.3; the exposition time $1 \mu s$, filter HC-9.

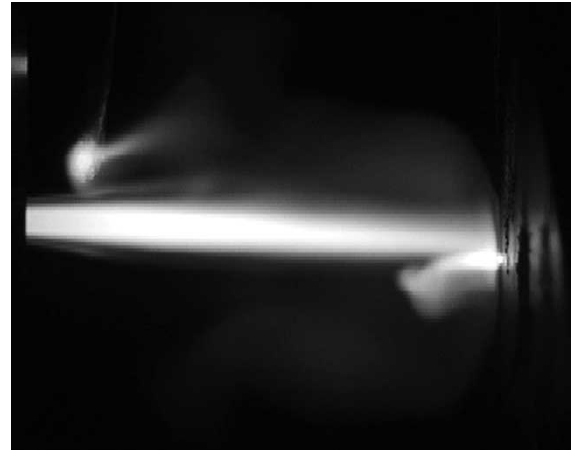
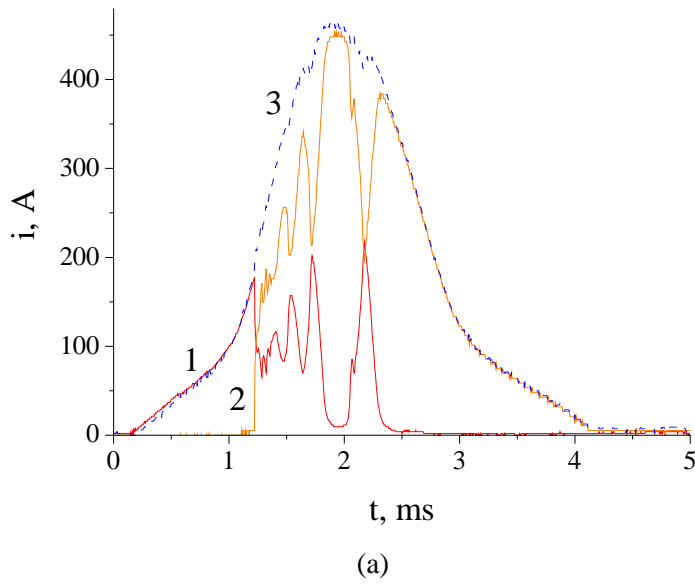


Fig. (12). (a) Current distributions in the case of grounded metallic target: (yellow curve) the target current, (red) the current in main circuit, (dashed) the sum current; $L = 6.87\text{mH}$, $d \approx 3\text{mm}$, $U = +1\text{kV}$, the distance to target $l = 28\text{mm}$. (b) TV-camera jet photo: $t_R = 1.08\text{ms}$, the exposition time $1\mu\text{s}$.

rather sharp bend. In practice, it coincides with the discharge current without the target. Thus, from the given series of experiments, it follows that a jet carries an electrical charge. The current behavior depends on the supply voltage polarity.

Also, we measure a floating potential of the target. Actually, we measure a potential difference Δu between the target and a ground. Value of Δu serves for potential estimation in a plasma jet. In this series of experiments we

had mainly the initial voltage of the storage battery $U = \pm 700\text{V}$. The distance l from capillary cut to the plate was changed in a range of $(20 - 212)\text{mm}$. The dark HC-10 filter was used. In Fig. (14a, b), the oscillograms of voltage for different distances l are presented. One can see, that the electric field arrives to a target surface with delay (an interval between discharge ignition and potential appearing at the target). A potential of the target grows sharply. At

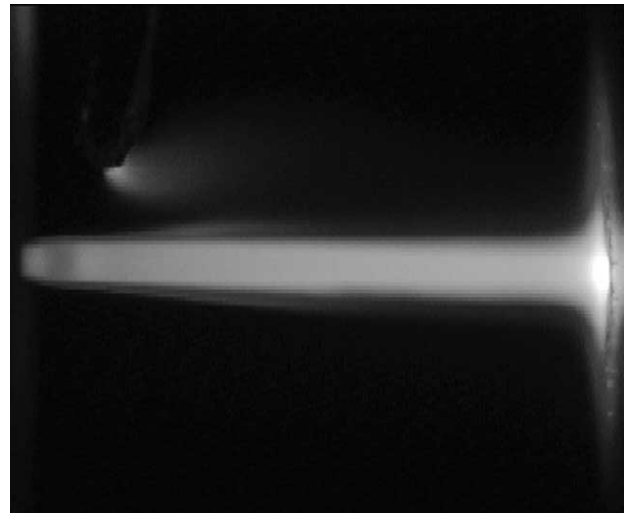
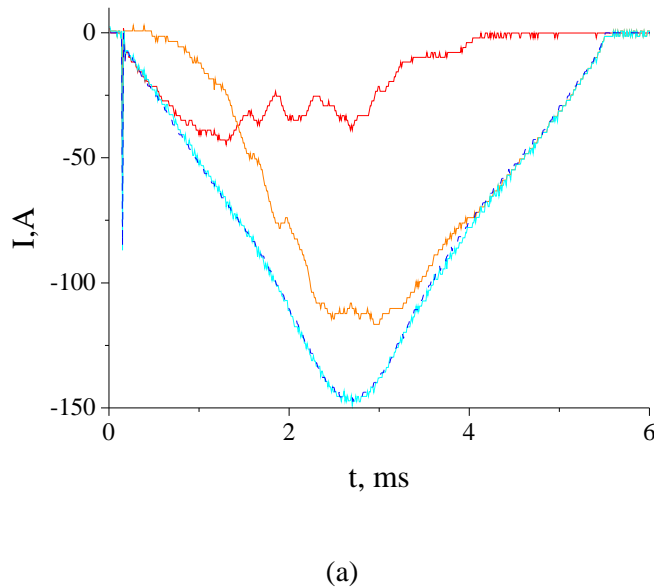


Fig. (13). (a) Current distributions in the case of grounded metallic target: (yellow curve) the target current, (red) the current in main circuit, (blue) the sum current; (dashed) the current in the free jet case; $L = 6.87\text{mH}$, $d \approx 1.5\text{mm}$, $U = -700\text{V}$, $l = 20\text{mm}$. (b) TV-camera jet photo: $t_R = 2\text{ms}$, the exposition $0.5\mu\text{s}$.

$U > 0$, the switch-off proceeds slower than the switch-on, being practically of the same as the current shape. At $U < 0$, the decrease in the potential occurs in the same manner as the switch-on and does not relate to the current shape. For $U > 0$ an average level of the target potential is in a range of $(40, 50) V$, and for $U < 0$ -- in a range of $(-40, -30) V$. At comparatively larger distances the potential level decreases strongly, having a deep oscillations (down to zero) at $U > 0$. Using the oscillograms of the target potential, the dependences of the moments t_r of potential appearing at the plate were built up (Fig. 15a) as well as the potential lifetime

Δt as a function of l (Fig. 15b). One can see that a straight line is fitted for the dependences $t_r(l)$ both at $U > 0$ and at $U < 0$, the slopes of both lines being practically equal. The line slope gives an estimation of velocity of potential front; it is $\approx 80 m/s$. This is velocity of the kernel propagation.

At higher initial voltage of storage battery ($U = \pm 1000 V$), qualitatively the same results were obtained, an average potential level being higher of about $20V$. Both dependences lying at the straight line, and velocity of potential front calculated *via* the slope increases up to $\approx 100 m/s$.

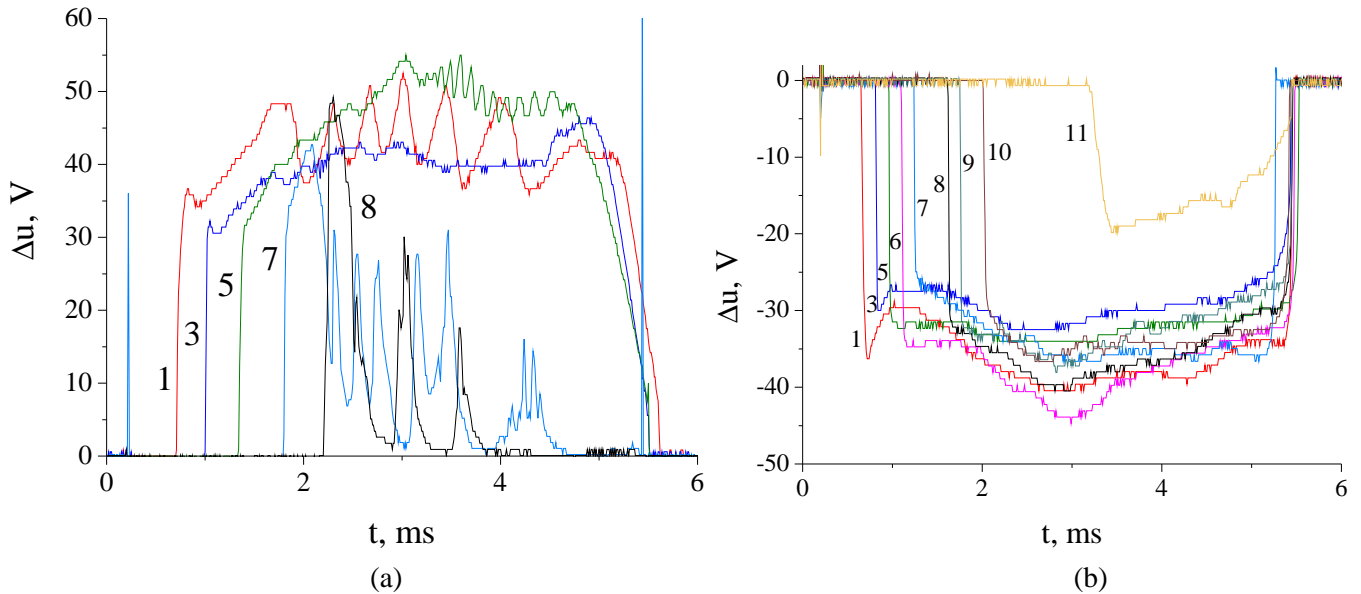


Fig. (14). Plots of the target voltage vs time for various target distances: (a) $U = +700V$, (b) $U = -700V$: (curve 1) $l = 20mm$, (3) 40, (5) 70, (6) 90, (7) 110, (8) 135, (9) 185, (10) 202, (11) 212.

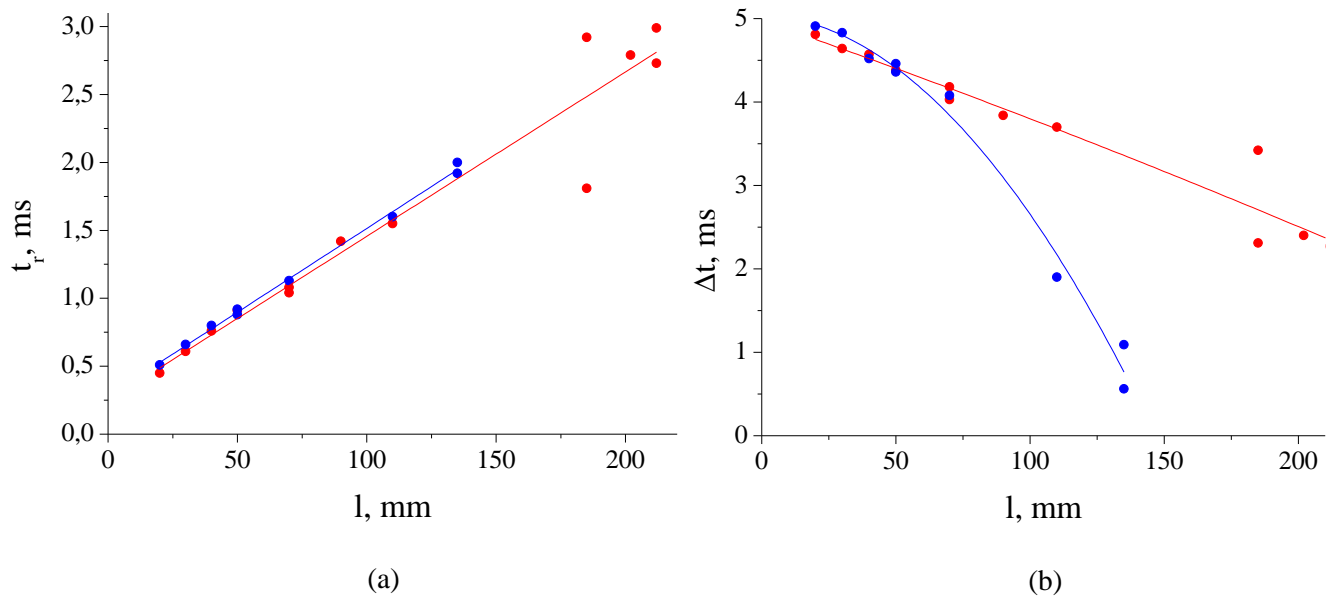
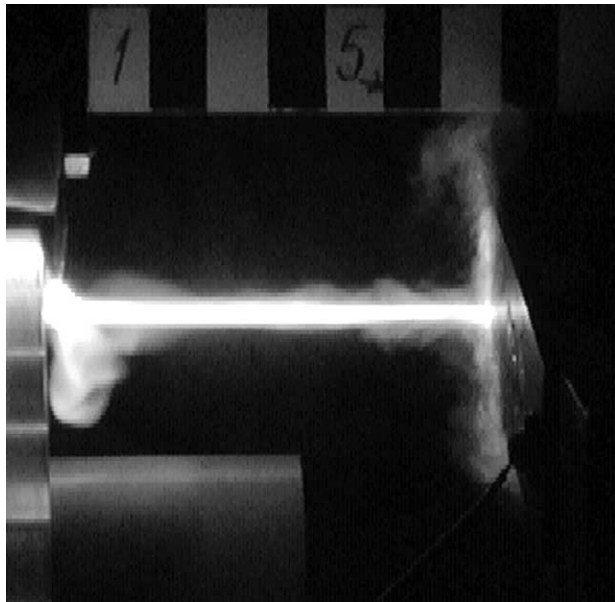
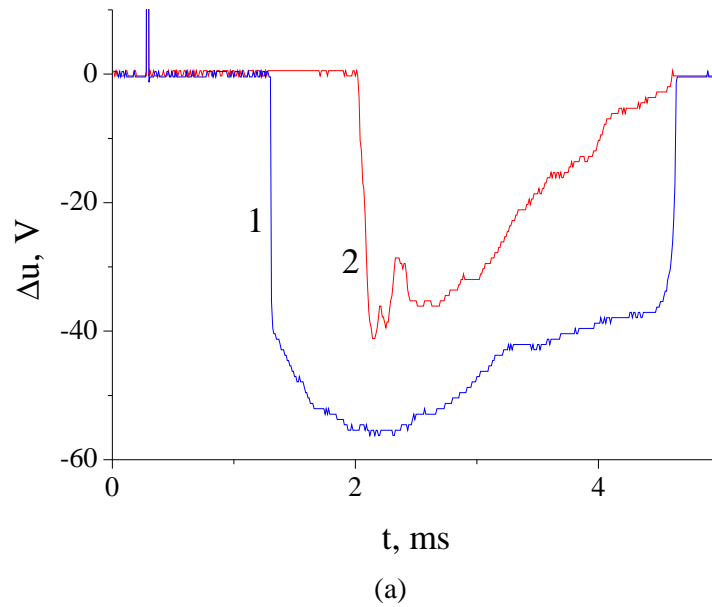
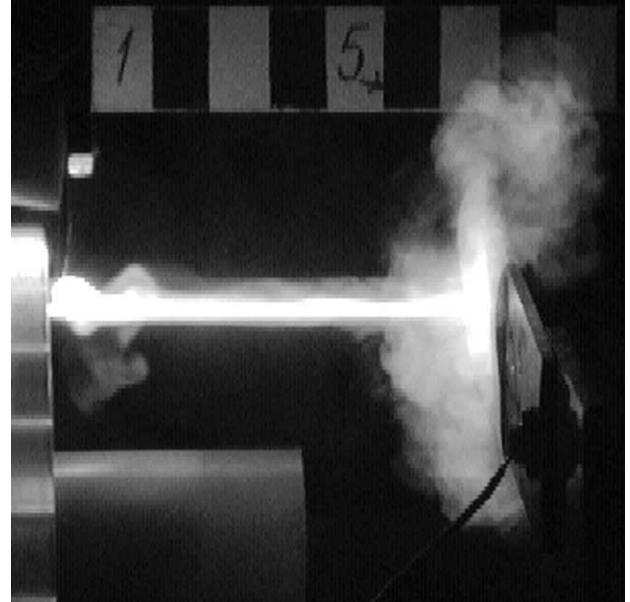


Fig. (15). Plots of (a) the moment of the potential appearing t_r and (b) the potential lifetime Δt at the target vs the distance to the target l . (Red circles) $U = -700V$, (violet squares) $U = +700V$. Approximation curves are obtained by the least-square method.



(d)



(e)

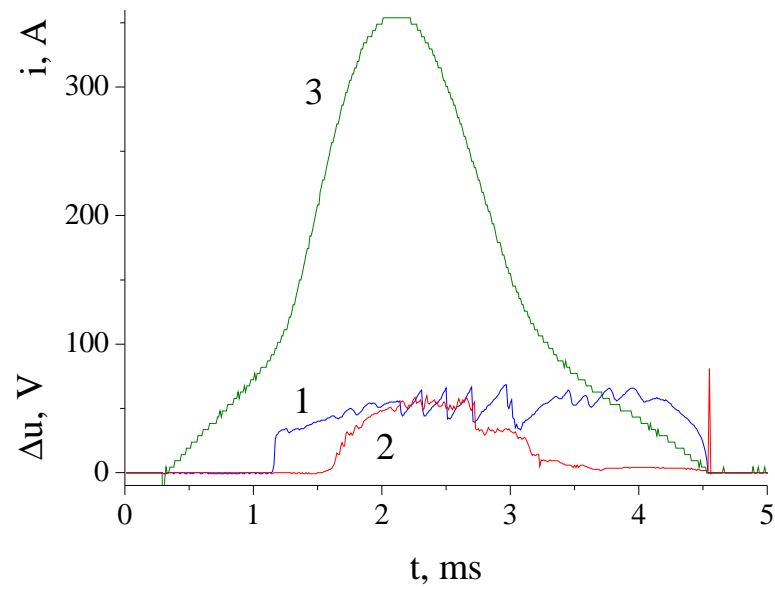
Fig. (16). (a) plots of the potential vs time: curve 1-- at the unprotected target, 2 -- at the target covered by paper. TV-photos of the jet: (b) for the unprotected target and (c) for the target with paper; $t_p = 2\text{ms}$, the exposition time $2\mu\text{s}$; $L = 6.87\text{mH}$, $d \approx 1.5\text{mm}$, $U = -1000\text{V}$; $l = 75\text{mm}$.

In Ref. [20], it was asserted that a paper or other dielectric located ahead of the plate protect it from heating and destruction. We study an effect of a plasma jet on the metal target which surface is covered by a writing-paper sheet of 80 g/cm^2 in density. The main effect consists in a $(0.5 - 1.0)\text{ms}$ delay in potential arising at the plate compared with the case without any paper (see, e.g., Figs. 16a, 17a). At the small distances of the target from the capillary cut, a paper is burned through by the first shot, and the larger distances, the darkening of paper occurs with no burn. The potential arising at the target does not depend on

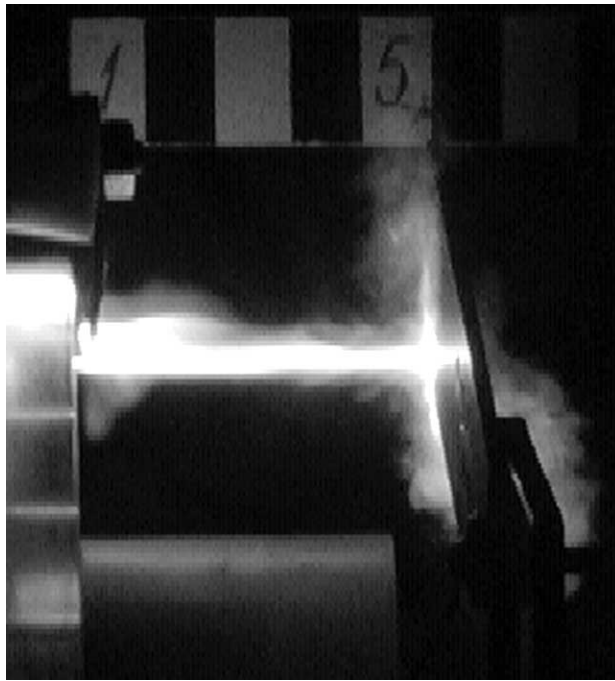
whether the paper is burned through or not. An average potential value being lower than without covering paper. The photos of relevant jet are shown in Figs. (16b, c, 17b, c). A jet shock on a paper creates a large cloud of condensed micro-particles.

6. JETS FROM NON-POLYMER CAPILLARIES

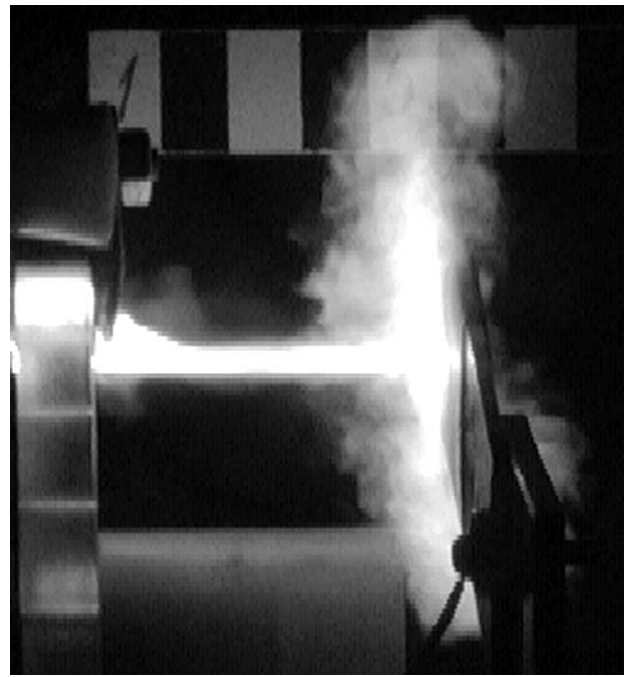
Earlier, it was supposed that the needle-like plasma jet can arise only when the capillary was made from any polymer [25]. Only in Ref. [29], a thin jet using a non-polymer capillary of BN was obtained. We also experimented with different non-polymer materials. A



(a)



(d)



(e)

Fig. (17). (a) plots of the potential vs time: curve 1 -- at the unprotected target, 2 -- at the target covered by paper, and curve 3 -- the main current vs time. TV-photos of the jet: (b) for the unprotected target, (c) for the target with paper; $t_e = 2\text{ms}$, the exposition time $2\mu\text{s}$; $L = 6.87\text{mH}$, $d \approx 1.5\text{mm}$, $U = +1000\text{V}$; $l = 50\text{mm}$.

changeable capillary from a *KCl* crystal was manufactured. Here, the atom masses of *K* and *Cl* are known and differ slightly (39.1 and 35.5). A rather thin jet arises. We estimated a value $q/\Delta m$. At a capillary diameter of 0.7mm , a single shot gives a loss of about 2.5mg in mass, a charge moved by jet is 0.3C , thus, $q/\Delta m \sim 120\text{C/g}$. Taking into consideration that the gram-equivalents of *K*

and *Cl* are about 39 and 35, $f = Mq/\Delta m$ is about $5 \cdot 10^3\text{C/mol}$. It can be compared with the relevant value estimated by us for the plexiglas for the same conditions. Analogous results we obtained for the capillary of *CsJ* crystal, too.

We also carried out the trial shots with a capillary in water ice. For this purpose, the water was frozen in a special

cuvette. A hole was drilled in the ice, then, the prepared capillary was inserted into a plexiglas body. The additional channels which were filled by liquid nitrogen to save the capillary in frozen state were drilled in this body. Discharge generates a thin jet from this capillary, too.

CONCLUSION

Thus, the losses in mass of capillary wall were accurately measured when the discharge proceeds. Also, the transferred charge was measured. It is shown that the ratio charge/mass multiplying the molar mass is comparable with the Faraday number. The velocity of plasma jet propagation was measured, too. It turned out to be about 100 m/s , being closed to the data of other authors. It was shown that the jet carries out a current from the capillary which is came back *via* a shell to the return electrode. It was found that the larger part of voltage drop involves the capillary and kernel and about (20–30)% refers to the shell. The current structure in plasma was studied, too. Our study revealed that a polarity of the plug electrode influences strongly the current distribution. As a rule, for the positive polarity, the whole current flows *via* grounded metal target, and for the negative one, only some portion of the current reaches the target. It was approved that a thin jet can be obtained not only from the polymer capillary but also from inorganic materials.

The present studies gave rise to a number of new possibilities of application of the capillary discharge with evaporated walls. Our first experiments showed that, a plasma jet can involve the dust particles of $50\text{ }\mu\text{m}$ size which hit in a glass resulted in deep craters. One way of investigation is to introduce the additional dust micro-particles with aim of studying their interaction with the jet as well as with various obstacles. These investigations are of importance for scientific purposes to study the jet dynamics itself and for applications concerning the dust interaction with airplane parts. Last year, this problem arose in relation with the activity of Eyjafjallajökull volcano in Iceland. In May 2011, another Iceland volcano became active. It is known that during the airplane flight through a cloud of volcanic dust, which deteriorates the air receivers resulting in blow-off of the engine and hits the windows resulting in their opacity. So, the study of interaction of a high-velocity jet of dust plasma with different targets is of high importance.

ACKNOWLEDGEMENTS

This work was supported in part by the Russian Foundation for Basic Research (projects N^o 09.08.01017 and N^o 10.08.00924) as well as the Federal program "Academic and teaching staff of innovative Russia in 2009-2013" (state contract N^o 02.740.11.0201).

CONFLICT OF INTEREST

None declared.

REFERENCES

- [1] Ogurtsova NN, Podmoshenskii IV. Investigation of a powerful pulsed discharge with a limited diameter of the channel. Opt Spectrosc 1958; 4: 725-7.
- [2] Ogurtsova NN, Podmoshenskii IV, Shelemina VM. Characteristics of the plasma jet of a powerful capillary discharge. Opt Spectrosc 1963; 15: 404.
- [3] Ogurtsova NN, Podmoshenskii IV, Shelepina VM. Continuous absorption coefficient of a Hydrogen-Carbon plasma at a temperature of 40,000 K and a pressure of Hydrogen of atmospheres. Opt Spectrosc 1964; 16: 514-8.
- [4] Ogurtsova NN, Podmoshenskii IV, Smirnov VL. Ohmic super-heating in the dense plasma of a capillary discharge. High Temp 1976; 14: 1-7.
- [5] Suckewer S, Jaeglé P. X-Ray lasers: past, present, and future. Laser Phys Lett 2009; 6: 411-36.
- [6] Burton RL, Turchi P. Pulsed plasma thruster. J Propul Power 1998; 14: 716-35.
- [7] Keidar M, Boyd ID, Beilis II. Model of an electrothermal pulsed plasma thrusters. J Propul Power 2003; 19: 424-30.
- [8] Keidar M, Boyd ID. Ablation study in the capillary discharge of an electrothermal gun. J Appl Phys 2006; 99: 053301.
- [9] Li BM, Kwok DY. Two-phase flow simulation of plasma-ignited combustion in an energetic fluid bed. J Plasma Phys 2004; 70: 225-35.
- [10] Li BM, Kwok DY. Multi-dimensional transient process for a pulse ablating capillary discharge: modeling and experiment. J Plasma Phys 2004; 70: 397-413.
- [11] Keidar M, Boyd ID, Beilis II. Ionization and ablation phenomena in an ablative plasma accelerator. J Appl Phys 2004; 96: 5420-8.
- [12] Cambier J-L, Young M, Pekker L, Pancotti A. Capillary discharge based pulsed plasma thrusters, preprint for presentation at the 30th IEPC. Florence Italy 2007; 238.
- [13] Chrisey DB, Hubler GK. Pulsed laser deposition of thin films. New York: Wiley 1994.
- [14] Bhuyan H, Favre M, Valderrama E, et al. Formation of sub-micron size carbon structures by plasma jets emitted from a pulsed capillary discharge. Appl Surf Sci 2009; 255: 3558-62.
- [15] Kukhlevsky SV, Kaiser J, Samek O, Liska M, Erotyak J. Stark spectroscopy measurements of electron density of ablative discharges in Teflon-(CF₂)_n capillaries. J Phys D: Appl Phys 2000; 33: 1090-92.
- [16] Keidar M, Boyd ID, Beilis II. On the model of Teflon ablation in an ablation-controlled discharge. J Phys D: Appl Phys 2001; 34: 1675-7.
- [17] Kozakov M, Kettlitz RM, Weltmann KD, Steffens A, Franck CM. Temperature profiles of an ablation controlled arc in PTFE: I. Spectroscopic measurements. J Phys D: Appl Phys 2007; 40: 2499-506.
- [18] Scheidenbach H, Uhrlandt D, Franke S, Seeger M. Temperature profiles of an ablation controlled arc in PTFE: II. Simulation of side-on radiances. J Phys D: Appl Phys 2007; 40: 7402-11.
- [19] Starikovskaia S M. Plasma assisted ignition and combustion. J Phys D: Appl Phys 2006; 39: R265-99.
- [20] Avramenko RF, Bakhtin BI, Nikolaeva VI, Poskacheva LP, Shirokov NN. A study of the plasma formations produced in an erosion discharge. Sov Phys Tech Phys 1990; 35: 1396-400.
- [21] Avramenko RF, Gridin AY, Klimov AI, Nikolaeva VI. Experimental study of energetic compact plasma formations. High Temp 1992; 30: 870.
- [22] Avramenko RF, Gridin AY, Klimov AI, Nikolaeva VI. Experimental investigation of the interaction of a high-enthalpy plasma with a shock wave and with high-power laser radiation. High Temp 1993; 31: 42-5.
- [23] Evans DA, Hardcastle MJ, Croston JH, Worrall DN, Birkinshaw M. Chandra and XMM-Newton observations of NGC 6251. Mon Not R Astron Soc 2005; 359: 363-82.
- [24] Bychkov VL, Gridin AY, Klimov AI. On the nature of artificial ball lightnings. High Temp 1994; 32: 179-83.
- [25] Bychkov AV, Bychkov VL, Timofeev IB. Experimental modeling of long-living radiant object produced from polymer organic materials in air. Khim Fiz 2006; 25: 89-97 (in Russian).
- [26] Tsui KH, Navia SE, Robba MB, Carneiro LT, Emelin SE. Self-similar magnetohydrodynamic model for direct current discharge fireball experiments. Phys Plasmas 2006; 13: 113503.
- [27] Leonov SB, Luk'yanov GA. On structure of the plasma jets from a pulsed erosive electro-discharge source. Prikl Mekh Tekh Fiz 1994; 35: 13-18 (in Russian).

- [28] Ershov AP, Timofeev IB, Shibkov VM, Chuvashov SN. On the kernel nature of capillary erosion discharge injected into air. *Vest Mosk U Fiz As* 1995; 36: 23 (in Russian).
- [29] Dimitrov SK, Zhdanov SK, Kirko DL, *et al.* Determining density and temperature of pulse plasma flow, and study of its structure. *Sib Fiz-Tekh Zh* 1992; 2: 57-60 (in Russian).
- [30] Muller L. Modelling of an ablation controlled arc. *J Phys D: Appl Phys* 1993; 26: 1253-9.
- [31] Bushman SS, Burton RL. Heating and plasma properties in a coaxial gasdynamic pulsed plasma thruster. *J Propul Power* 2001; 17: 959-66.
- [32] Dorodnov AM, Petrosov VA. Physical principles and types of technological vacuum plasma devices. *Sov Phys Tech Phys* 1981; 26: 304-15.

Received: August 15, 2011

Revised: October 11, 2011

Accepted: October 13, 2011

© Ender *et al.*; Licensee *Bentham Open*.

This is an open access article licensed under the terms of the Creative Commons Attribution Non-Commercial License (<http://creativecommons.org/licenses/by-nc/3.0/>) which permits unrestricted, non-commercial use, distribution and reproduction in any medium, provided the work is properly cited.